Jurnal
Teknologi

Full Paper

ENERGY CONSUMPTION REDUCTION OF A MULTI-CIRCUIT CENTRALIZED AIR CONDITIONING SYSTEM USING PID CONTROL

Ibrahim Oleolo[a*], Hayati Abdullah[a], Maziah Mohamad[a], Samuel Moveh[b], Emmanuel Alejandro Merchán-Cruz[b], Abiodun Emmanuel Abioye[c]

[a]School of Mechanical Engineering, Faculty of Engineering, Universiti Teknologi Malaysia, 81310 UTM Johor Bahru, Johor, Malaysia
[b]Transport and Telecommunication Institute, LV-1019 Riga, Latvia
[c]Electrical Engineering, Reedley College, California, USA

Article history
Received
15 March 2025
Received in revised form
14 July 2025
Accepted
14 July 2025
Published Online
27 February 2026

*Corresponding author
olakunle1983@graduate.utm.my

Graphical abstract

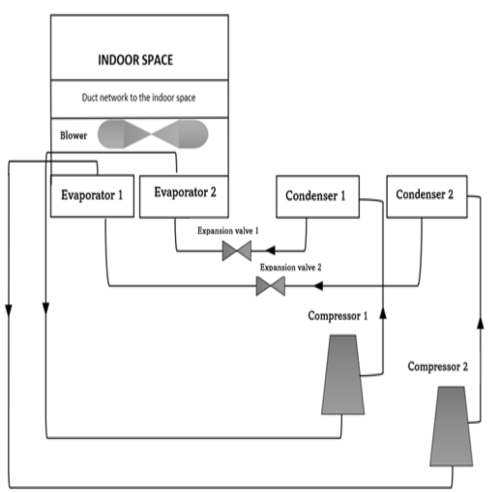

Abstract

The increased use of air conditioning systems have a great effect on a building's overall energy consumption. An energy reduction plan that can at the same time guarantee thermal comfort is necessary for efficient energy management in air conditioning systems. The centralized type air conditioning systems are mostly used in commercial buildings. Most of them have constant speed compressors installed, which consume about 90% of the energy used by the air conditioning system. Therefore, reducing the energy consumption of the compressor is a practical way to regulate the energy of the air conditioning systems. Very few studies were carried out involving operational centralized multi-circuit air conditioning system, and those that have been conducted are restricted to water-cooled package units. This paper presents a study on the application of PID control system utilizing variable frequency drive technology on an installed and operational multi-circuit centralized air cooled air-conditioning system. The PID implementation was compared with the On/Off control's baseline energy usage. The results obtained showed that the PID was able to save 35.7%, 38.8% and 40.3% of energy consumption at temperature setpoints of 23°C, 24°C, 25°C respectively. This study has contributed towards the development of an advanced control strategy that has resulted in the reduction of energy consumption and improvement in the performance of an operational multi-circuit centralized air conditioning system.

Keywords: Air conditioning, control, energy, multi-circuit

Abstrak

Peningkatan penggunaan sistem penyaman udara mempunyai kesan yang besar terhadap penggunaan tenaga keseluruhan bangunan. Pelan pengurangan tenaga yang boleh pada masa yang sama menjamin keselesaan terma adalah perlu untuk pengurusan tenaga yang cekap dalam sistem penyaman udara. Oleh itu, mengurangkan penggunaan tenaga pemampat adalah cara praktikal untuk mengawal tenaga sistem penyaman udara. Sangat sedikit kajian telah dijalankan melibatkan sistem penyaman udara berbilang litar berpusat operasi, dan yang telah dijalankan adalah terhad kepada unit pakej yang disejukkan dengan air. Kertas kerja ini membentangkan kajian tentang aplikasi sistem kawalan PID menggunakan teknologi pemacu frekuensi berubah-ubah pada sistem penghawa dingin berpusat berpusat berbilang litar yang dipasang dan beroperasi. Keputusan yang diperolehi menunjukkan bahawa PID mampu menjimatkan penggunaan tenaga sebanyak 35.7%, 38.8% dan 40.3% pada titik tetapan suhu masing-masing 23°C, 24°C, 25°C. Kajian ini telah menyumbang ke arah pembangunan strategi kawalan lanjutan yang telah menghasilkan pengurangan penggunaan tenaga dan peningkatan dalam prestasi sistem penghawa dingin berpusat berbilang litar operasi.

1.0 INTRODUCTION

With a growing population, the world's energy use is increasing significantly due to an increase in energy usage. Because of this increase in energy demand and the depletion of existing fossil fuel supplies, more sufficient energy consumption is needed to balance the world's energy requirements [1]. Researchers have made attempts to achieve efficiency in energy utilization. About half of the total energy consumption of modern society is used in buildings, making it one of the largest users of energy in the world. As the population keeps growing and energy demands keep increasing, the building sector energy requirement accounting for about 40%, keeps growing and it is forecasted to increase to about 50% in this year 2025 [2], [3], [4], [5]. The major part of the building energy consumption is for Heating, Ventilation and Air Conditioning (HVAC) [6], [7]. Studies have shown that 50% of the building energy use, is being consumed by HVAC equipment in industrial and commercial buildings [3], [4]. This can be seen from the increasing prevalence of the number of systems used for air conditioning. As a result, the increased use of air conditioning has had a major effect on total energy consumption. Heat is transferred from the air inside the air conditioning space to the outside air by the air conditioning systems. Heat is first transmitted from the evaporator to the refrigerant and subsequently from the refrigerant to the condenser. In this instance, pushing the refrigerant from the evaporator to the condenser is greatly aided by the compressor. About 90% of the energy used in an air conditioning system is used by the compressor, which is the primary energy consumer [8]. Centralized air conditioning systems with direct expansion are frequently utilized in commercial buildings. Most of these systems use the traditional on/off control approach, which keeps the compressors operating at a steady speed [2]. This always results in maximum capacity for cooling and this makes indoor room to overcooled in some situations. This usually results in wasting energy and causing discomfort, especially when the cooling load is low. This usually occur in both single and multi-circuit refrigeration system. One of the methods investigated and used to preserve thermal comfort of a conditioned space while reducing energy consumption is the Variable Frequency Drive (VFD) of compressor [9], [10]. The VFD technology allows HVAC system to adjust its output capacity according to the conditioned space temperature demand, which has provided many opportunities for improved temperature control and energy consumption savings. Thus, the capacity control through compressor speed modulation by varying the frequency drive of the motor of the compressor ensures that the system output cooling capacity is matched with the varying cooling load of the conditioned space. Many VFD technologies focus on a single circuit air-conditioning systems like domestic and small-scale office applications comprising only tests on a laboratory rig. Very little work is done on medium or large-scale multi-circuit package air conditioning systems [2], [11], [12]. Therefore, it is the focus of this study to further research on the concept of variable frequency drive of compressor in the Multi-Circuit Centralized air cooled air-conditioning system. Multiple refrigerant circuit systems offer a certain amount of flexibility during a capacity control. For example, an additional circuit could be provided for a multi-circuit refrigerant system to provide a degree of overcapacity with respect to a building's usual cooling demand. Any or more refrigerant circuits may be shut down at times of normal cooling demand, with the remaining circuits having sufficient capacity to meet the cooling demand. The additional refrigerant circuit is enabled when the need arises, such as on hot and humid days, whereby the thermal indoor requirement might be high and the device can now meet the increased cooling requirements. But to provide the required cooling demand, it is costly to install a separate refrigerant circuit with its attendant components, capacity management is provided through a phase increase, not a desired continuous variable increase, and one or more refrigerant circuits must be selectively and regularly activated or deactivated. Thus, this paper analyses the application of VFD to the operation of a Multi-Circuit Centralized air cooled air-conditioning system.

2.0 METHODOLOGY

The experimental work was carried out at Block D06, language academy Universiti Teknologi Malaysia. The two-circuit refrigerant air-cooled package unit was installed inside the AHU within the building. It is operated between 8:00 am - 5:00pm Sunday to Thursday which are the official days in the state of Johor, Malaysia. The office space that is served by the system is located beside the AHU. It is supplied with cooled air through the ducting network which connects the system to the indoor space. The office is operated between 8:00am–5:00pm. The air-conditioning system base case set point temperature was 24°C. The schematic floor plan of block D06 is shown in Figure 1. The multi-circuit configuration is useful as it provides alternative capacity when there is failure of one of the refrigerant circuits. The air conditioning system used in this study is the Multi-circuit centralized air cooled air-conditioning system consisting of:

1) Two Independent Refrigeration Circuits

Multi-circuit concepts are often employed in air conditioning and refrigeration systems to enhance reliability, efficiency, and flexibility. Since each circuit runs separately, the system can continue to function even in the event that one circuit fails [13]. It offers a backup system, which is vital for settings like data centers, hospitals, and some industrial processes where reliable temperature management is required. Each refrigeration circuit is a vapor compression cycle where the refrigerant enters the compressor as a vapor. Each refrigerant circuit includes a compressor, a condenser, an expansion device and an evaporator connected in the refrigeration circulation flow. The two independent refrigeration circuits provide partial capacity in case of failure of any of the compressors [2], [4], [14]. Figure 2 shows the schematic of the two-refrigeration circuits air conditioning system

2) Air Distribution Sub-System

The air distribution sub-system in a centralized air conditioning system plays a vital role in delivering conditioned air efficiently and maintaining a comfortable and healthy indoor environment [1], [15]. Proper design, installation, and maintenance of this subsystem are essential for optimal performance and energy efficiency. It has the duty of distributing cooled air from the central unit to different areas of a building. This subsystem is essential to preserving comfort, temperature management, and indoor air quality. The air distribution sub-system consists of:

- Air distribution duct network with supply, return and outdoor air duct.
- Blower section with centrifugal supply fan
- Air-conditioned space (Indoor)
- Air handling unit (AHU)

Ensuring the system is balanced and functioning correctly is critical for performance[16]. Professional commissioning involves testing and adjusting the system to ensure proper airflow and temperature distribution. The field measurement, data collection and procedure for both indoor and outdoor in this study is implemented in same procedure as in [2]. In [2], the control method was implemented in a centralized water-cooled package unit

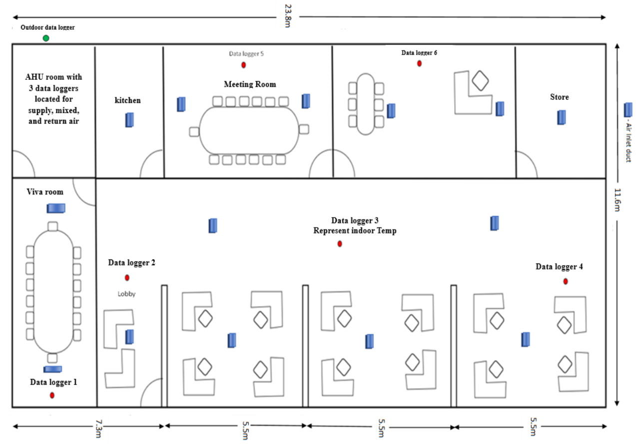

Figure 1 Schematic layout of the indoor space environment

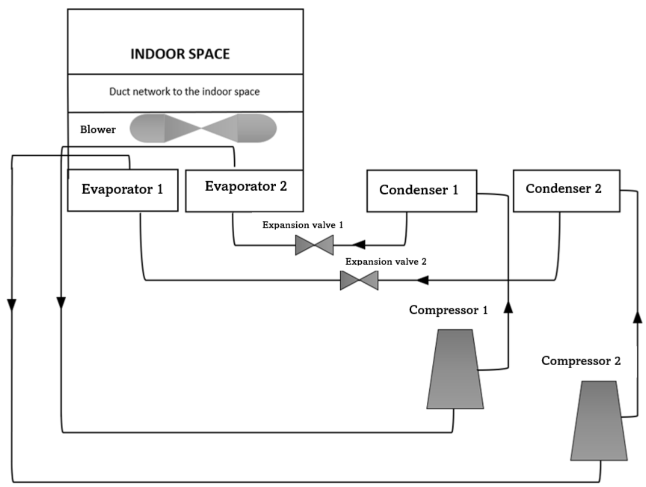

Figure 2 Two refrigeration circuits units with one blower

An essential part of heating, ventilation, and air conditioning (HVAC) systems that regulate and circulate air around buildings is an Air Handling Unit (AHU) [1]. AHUs are essential for preserving indoor comfort and air quality and are present in both residential and commercial buildings. It moves air through the ductwork of the structure, supplying conditioned air to different rooms and spaces. AHUs regulate air temperature by heating or cooling it using heating coils or cooling coils connected to a boiler, chiller, or heat pump air from the building's interior space is drawn into the return air ducts and returned back to the AHU. At the same time, fresh outside air from the surroundings is drawn into the AHU to mix with the returned air. The warm mixed air then enters the evaporator where the warm air is being cooled. This cooled air is then supplied through the supply air duct to the indoor office space. Figure 3 shows the pictures of the AHU.

(a) Power and Control unit

(b) Multi-circuit Air conditioning unit

Figure 3 Pictures of the AHU room

A. Simulation Framework of the Multi-Circuit Centralized Air Conditioning System

The simulation framework for the multi-circuit air conditioning system is shown in Figure 4. The multi-circuit air conditioning system is represented by the compressor 1, compressor 2 and the disturbance model.

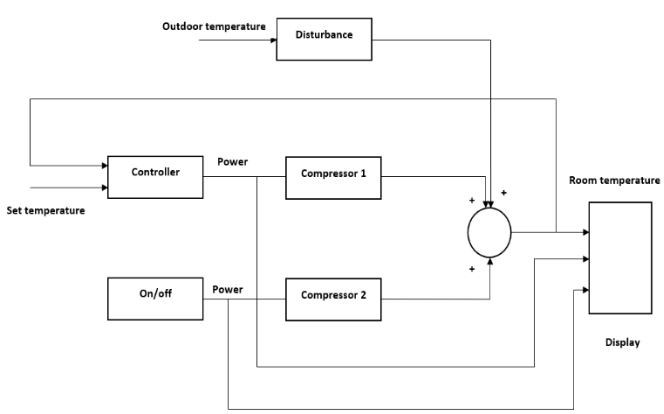

Figure 4 Simulation framework

The transfer functions for the compressors 1 and 2 were modelled and are given in Equations 1 and 2 respectively.

$$G_1(z) = \frac{-0.00000113z^{-1} + 0.00000389z^{-2} - 0.000003389z^{-3} + 0.000001132z^{-4}}{1 - 3.998z^{-1} + 5.994z^{-2} - 3.994z^{-3} + 0.9979z^{-4}} \quad (1)$$

$$G_2(z) = \frac{-0.000007366z^{-1} + 0.00002194z^{-2} - 0.00002178z^{-3} + 0.000007207z^{-4}}{1 - 3.979z^{-1} + 5.939z^{-2} - 3.94z^{-3} + 0.9801z^{-4}} \quad (2)$$

The controller used in this study is the Proportional Integral and Derivative (PID) controller.

B. PID Controller Design

A Proportional Integral and Derivative (PID) controller is a control loop feedback mechanism widely used in industrial control systems to maintain a desired output setpoint. It combines three distinct control strategies: proportional, Integral, and Derivative, to provide precise and stable control of a process [17]. The PID algorithm is a popular feedback control system which has been used in many applications and industries. It is a robust and easily understood algorithm that can provide excellent control performance despite the varied dynamic characteristics of the system. It consists of three basic modes, Proportional (P), Integral (I) and derivative (D), which signifies the present error, past error and future error respectively. According to Equation 3, the variable e(t) represents the error which is the difference between the desired input and actual output. The Proportional, Integral and Derivative parts of the controller perform different tasks in the whole control process and generate control signal u(t) to the plant as in Figure 5. The kp, ki and kd represent the control action, which are proportional gain, integral gain, and derivative gain respectively.

$$u(t) = k_p e(t) + k_i \int_0^t e(t)dt + k_d \frac{de(t)}{dt} \quad (3)$$

The Block diagram of the PID closed loop control system is shown in Figure 5.

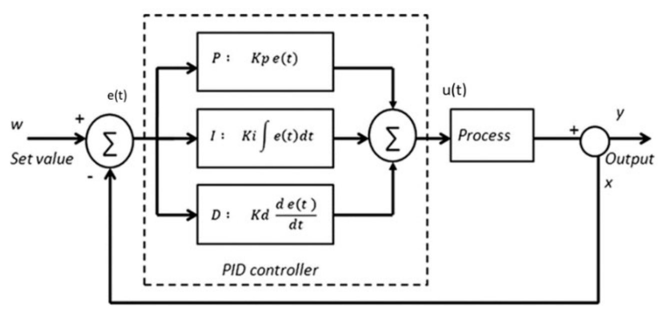

Figure 5 Block diagram of a PID control system

The Simulink block diagram for the PID controller is shown in Figure 6. The PID controller was tuned using manual tuning, auto tuning and Ziegler Nichols tuning method.

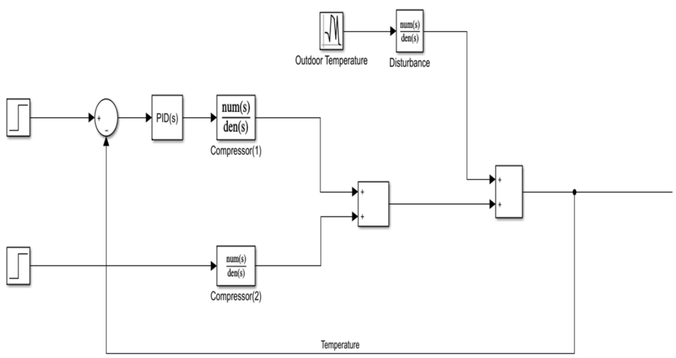

Figure 6 Simulink Block diagram for PID Controller

The following sections present the results and discussion for the PID tuning and simulation using the auto, manual and Ziegler Nichols tuning method

A. Ziegler–Nichols Tuning

A popular method for tuning P, PI, and PID controllers is the Ziegler–Nichols method. Ziegler–Nichols method of tuning is suitable for a regulatory system. The Ziegler–Nichols tuning method is a heuristic method of tuning a PID controller. It is performed by setting the I (integral) and D (derivative) gains to zero. This tuning rule is meant to give PID loops the best disturbance rejection. The Zeigler–Nichols's method is based on the frequency response of the closed loop system in which the gain is increased until the closed loop system becomes stable [17]. While using the proportional control action only as in Figure 7, K_p is increased from 0 to a critical value K_{cr} at which the output first exhibits sustained oscillations. Thus, the critical gain K_{cr} and the corresponding period P_{cr} are experimentally determined, as shown in Figures 8 and 9. Ziegler–Nichols suggested that the parameters K_p, τ_i, and τ_d are set according to the formula shown in Table 1.

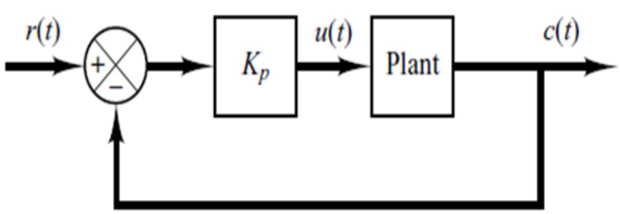

Figure 7 Proportional control

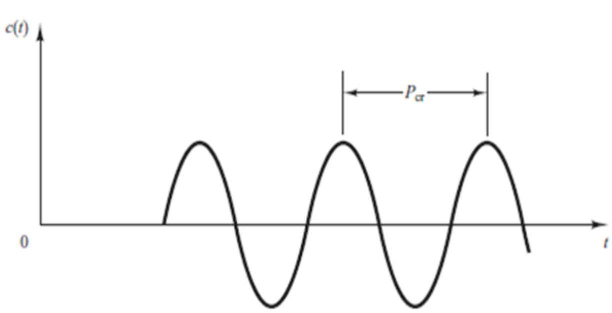

Figure 8 Corresponding period P_{cr}

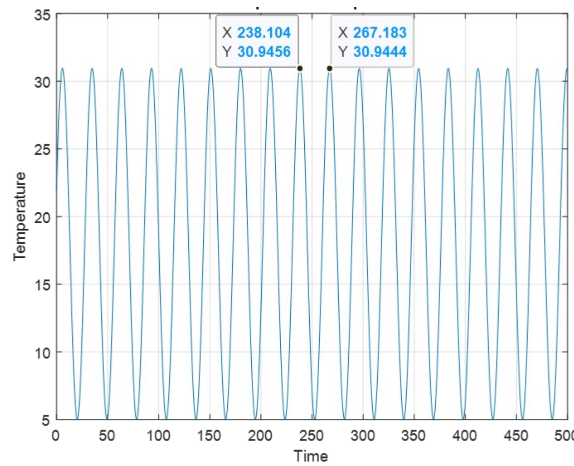

Figure 9 Temperature response

The values for the Ziegler–Nichols tuning rule based on critical gain K_{cr} and critical period P_{cr} are given in Table 1.

Table 1 Ziegler–Nichols Tuning Rule

Ziegler-Nichols	K_p	τ_I	τ_D
P	$0.5K_{cr}$	-	-
PI	$0.45K_{cr}$	$P_{cr}/1.2$	-
PID	$0.6K_{cr}$	$P_{cr}/2$	$P_{cr}/8$

Figure 10 shows the block diagram implemented in MATLAB/Simulink to find the ultimate gain K_{cr}.

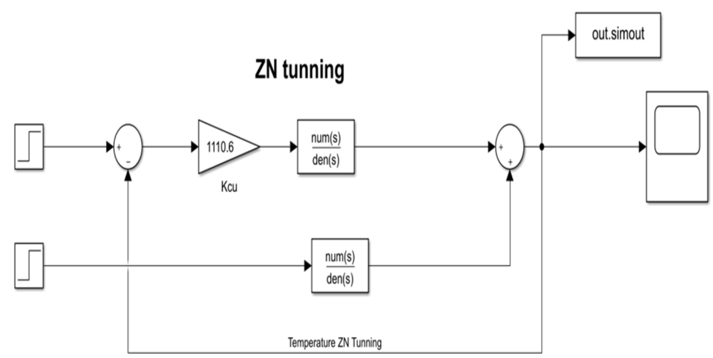

Figure 10 Simulink Diagram to find the ultimate gain $\boldsymbol{K_{cr}}$

Using K_{cr}=1110.6, and calculating P_{cr}=267.183 - 238.104 =29.0790 from Figure 10, the values for the PID controller can be calculated using Table 1

$$K_p = 0.6K_{cr} = 0.6(1110.6) = 666.36$$

$$\tau_I = \frac{P_{cr}}{2} = \frac{29.0790}{2} = 14.5395$$

$$\tau_D = \frac{P_{cr}}{8} = \frac{29.0790}{8} = 3.6349$$

Finally, the PID controller gains are calculated as shown Equation 4:

$$G_c = 666.36 + \frac{45.8310}{s} + 2422.2s \quad (4)$$

K_p=666.36
K_i=45.8310
K_d=2422.2

With these values, an unstable response was achieved, because the K_i gain is large. The gain K_i was adjusted as, K_i=2.8310.

The plot of the tuning operation on the PID parameters for the three method is presented in Figure 11. The tuning was done at 23°C setpoint. From the plots, the parameters tuned from manual tuning gives the best performance, it has a lower overshoot and a faster stability.

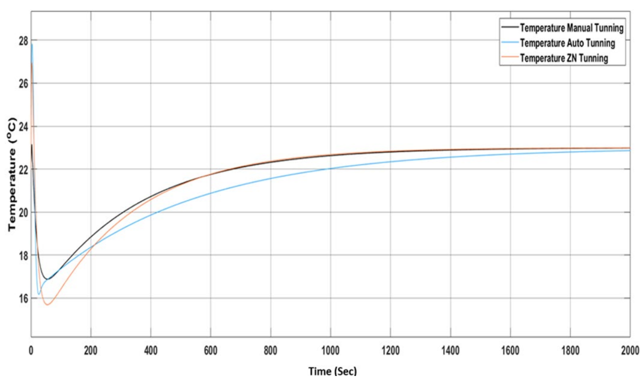

Figure 11 Tunning result at 23°C for the three method

The results of the tuning operation on the PID parameters at 23°C is summarize in Table 2 and 3, the parameters derived from manual tuning gives the best performance having the lowest settling time and overshoot.

Table 2 PID Performance

Tunning Method	Settling Time (Min)	Overshoot (%)
Ziegler–Nichols	35	19.6
Manual	32	10
Auto	43	28.1

This PID parameters for manual tunning at 23°C as presented in Table 3 was used in the real implementation on the centralized multi circuit air conditioning system

Table 3 PID Controller Gains

Parameter	Tuned Value
K_p	800
K_i	3
K_d	2

B. PID Controller Implementation

The operating principle between the two compressors is established according to the following algorithm for the PID control based on the feedback from the indoor space air temperature through the thermocouple

ALGORITHM
If $T_{IN} \leq (T_{SP} + 0.3)$
Compressor 1: variable speed
Compressor 2: off
else If $T_{IN} \geq (T_{SP} + 0.6)$
Compressor 1: maximum speed
Compressor 2: on
else Compressor 1: variable speed
Compressor 2: off
end
where
T_{SP} = Setpoint
T_{IN} = Feedback from indoor space air temperature

The overall strategy ensures stable temperature setpoint, reduction in energy performance and better performance when compared to the On/Off thermostat control of the base case. Figure 12 shows the schematic diagram of the control structure of the PID and On/Off control implemented at the AHU.

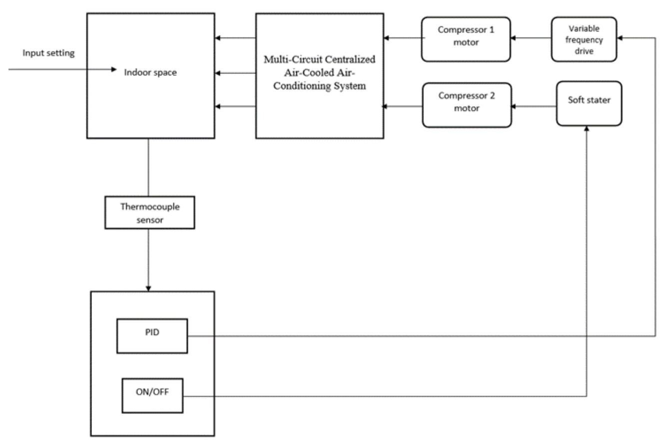

Figure 12 PID control structure

C. Variable Frequency Drive Installation

Variable Frequency Drive (VFD) is a type of motor controller that controls the electric motor by varying the frequency and voltage supplied to the electric motor, such that the speed supplied matches what is required at a particular point in time, to prevent unnecessary waste of energy. It is also known as variable speed drive [18]. The VFD is composed of a three-phase AC induction motor and a variable frequency power supply. The variable frequency power supply uses solid state components to produce a modulated pulse-width current that varies with both the voltage and frequency transmitted to the motor [18]. It allows for accurate control over a wide range of motor speeds. The first stage of a variable frequency drive is the conversion of the 3 phase AC signals to DC signals by a rectifier. The next stage is the DC intermediate circuit which contains the capacitor for filtering the current to produce a smooth and clean DC signal. In the last stage, the inverter converts the smooth DC current back to AC current and supply to the motor as required. Figure 13 shows the schematic diagram of the working principle of a VFD. In this study, the ABB drive was installed and is connected to the motor of the compressor 1 of the air conditioning unit.

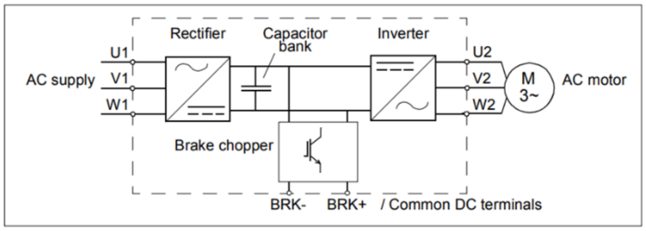

Figure 13 Circuit diagram of the variable frequency drive

D. Soft Starter Installation

A soft starter is an accessory that can be attached to a motor to enable the motor to employ a different manner of startup. It permits a more gentle and effortless power-up of the motor and restricts the amount of voltage that can surge through it. This device is designed to lessen the pressure placed on the motor during the regular power-up phase of a motor. The soft starter when installed, gradually begins applying increasing voltages to the motor instead of a sudden rush of voltage. It does this by limiting the torque in the motor. This allows for smooth acceleration of power as the sudden rush of voltage frequently can cause great damage to the motor. The working principle of a soft starter reduces the overall wear and tear of the motor, thus increasing its life span. Soft starters are made up of mechanical, electrical, or both types of mechanisms. Clutches and various coupling types that use a fluid, magnetic forces, or steel shot to limit torque are examples of mechanical soft starts. Any control system that briefly lowers the voltage or current input to lessen torque, or a device that momentarily changes how the motor is linked in the electric circuit, can be an electrical soft starter. The ABB compact range model was installed in this study and it was connected to compressor 2. This model can handle more than 20 starts per hour. Figure 14 shows the circuit diagram of the soft starter

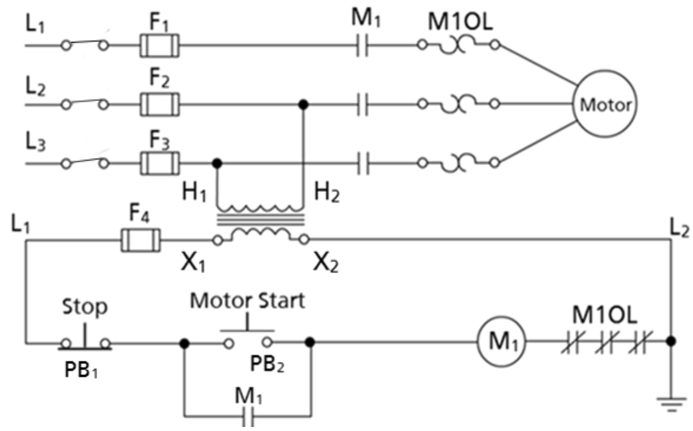

Figure 14 Circuit diagram of the ABB soft starter

The photographs of the PID controller, soft starter and variable frequency drive are shown in Figure 15. Figure 15a shows the front view of the controller, while Figure 15b shows the wiring connections of the variable frequency drive, soft starter, and thermocouple to the controller. Figure 15c and Figure 15d show the VFD and soft starter respectively.

(a) PID controller

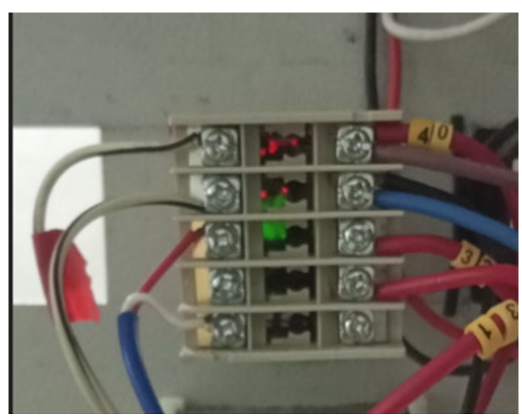

(b) PID controller wiring

(c) Variable frequency drive for compressor 1

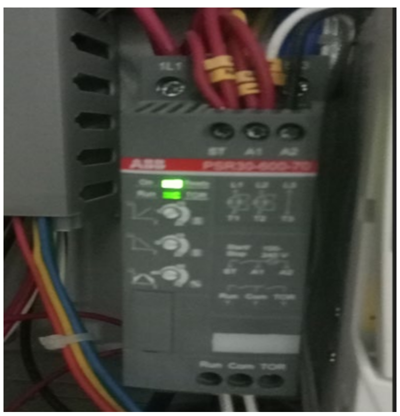

(d) Soft starter for compressor 2

Figure 15 PID control implementation in the AHU

3.0 RESULTS AND DISCUSSION

In the following sections, the results of the effect of the controllers after installation are presented. The energy consumption for the PID controller is calculated and compared with the on/off base case to determine the energy savings and the coefficient of performance. Analysis of the setpoint tracking is also presented.

A. Energy Consumption Analysis

The hourly energy consumption for 23°C, 24°C and 25°C setpoints for the On/Off and PID controllers were determined and the results are presented below. The power consumption of the compressor is an important parameter in determining the performance of an air conditioning system. The system is installed with two scroll type compressors. The CW240 power analyzer was used to measure the power consumption of the compressors. This power analyzer has a display which provides measurement for voltage, current and electric power. Figure 16 shows the Yokogawa Clamp-on Power Analyzer IM CW240E model.

Figure 16 Power Analyser to measure energy consumption

The energy consumption for 23°C, 24°C and 25°C setpoints for the On/Off, and PID controllers were determined. The energy savings is calculated after implementation of the PID. This is to show the effect of the PID strategy on the multi-circuit centralized air conditioning system, when compare to the On/Off base case. This calculation is done for the three setpoints of 23°C, 24°C, 25°C based on Equation 5.

$$\text{Energy savings} = \frac{\text{Total On/Off energy consumption} - \text{Total PID energy consumption}}{\text{Total On/Off energy consumption}} \times 100 \quad (5)$$

The above formula give rise to the energy savings results as indicated in Tables 4, 5 and 6, by comparing the effect of PID with the On/Off base case for the three temperature setpoints. The daily energy consumption at 23°C, 24°C and 25°C setpoints for the On/Off and PID controls are as shown in Table 4. The energy savings at the three setpoint after implementation of PID is shown in Table 5. The hourly average energy consumption is shown in Table 6.

Table 4 Daily (9:00am- 4:00pm) daily Energy Consumption

	On/Off		PID	
	Date	**Daily Energy Consumption (kwh)**	**Date**	**Daily Energy Consumption (kwh)**
	18/04/2021	126.1	26/12/2021	80.3
	19/04/2021	122.0	27/12/2021	80.5
23°C	20/04/2021	125.2	28/12/2021	78.4
	21/04/2021	122.5	29/12/2021	80.1
	22/04/2021	122.9	30/12/2021	78.3
	Total Energy Consumption (kwh)	**618.8**	**Total Energy Consumption (kwh)**	**397.6**
	20/10/2019	115.7	2/1/2022	70.4
	21/10/2019	114.5	3/1/2022	70.1
24°C	22/10/2019	113.9	4/1/2022	70.0
	23/10/2019	116.7	5/1/2022	68.5
	24/10/2019	115.8	6/1/2022	73.9

	Total Energy Consumption (kwh)	576.7	Total Energy Consumption (kwh)	353.1
	29/03/2021	112.7	16/1/2022	67.5
	30/03/2021	110.4	17/1/2022	67.0
25°C	31/03/2021	110.5	19/1/2022	66.3
	01/04/2021	111.7	20/1/2022	65.7
	04/04/2021	111.4	23/1/2022	65.4
	Total Energy Consumption (kwh)	556.7	Total Energy Consumption (kwh)	331.9

Table 5 summarized the energy savings for the three temperature setpoints in kWh and percentage as derived from Table 6

Table 5 Energy Savings after PID Implementation

Temp Setpoint	On/Off	PID	Energy Savings (kWh)	Energy Savings (%)
23°C	618.8	397.6	221.2	35.7
24°C	576.7	353.1	223.6	38.8
25°C	556.7	331.9	224.8	40.3

From the above results it can be observed that the application of PID to the multi-circuit centralized air conditioning system resulted in energy savings of 35.7% at 23°C, 38.8% at 24°C and 40.3% at 25°C.

B. Coefficient Of Performance

The coefficient of performance of the air conditioning system is the ratio of the rate of net heat removal to the rate of total energy input. A high COP value represents a high efficiency. The COP is a parameter that affects the efficiency and energy consumption of the air conditioning system. Equations 6 is used to calculate the COP for the On/Off and PID controllers at 23°C, 24°C, 25°C setpoints on an hourly basis for each day. Table 7 shows the summary of the results for the average daily COP for all the three controllers at the three different temperature setpoints of 23°C, 24°C, and 25°C.

$$\mathrm{COP} = \frac{\text{Rate of net heat removal (Cooling Capacity, } Q_{cc})}{\text{Rate of total energy Input } (W_{input})} \quad (6)$$

$$Q_{cc} = \text{Sensible Heat} + \text{Latent Heat} = Q_s + Q_L \quad (7)$$

According to ASHRAE standard [19], the sensible heat and latent heat can be calculated as follows:
The sensible heat gain corresponding to the change in the dry-bulb temperature, ΔT for a given air flow, is determined by Equation 8.

$$Q_s = (\text{mass flow rate of supply air}) \text{ x } (\text{specific heat capacity}) \text{ x } (\text{temperature change})$$

$$Q_s = \dot{m} \text{ x } c \text{ x } \Delta T \quad (8)$$

Where:
$\dot{m}$ = mass flow rate of supply air
ΔT = (Temperature of mixed air – Temperature of supply air)
c = specific heat capacity of dry air and water vapour
While the Latent Heat, Q_L can be calculated as in Equation 9.

Latent heat gain = (mass flow rate of supply air in kg dry air per second) x (change in humidity ratio) x (latent heat of evaporation in kJ per kg moisture)

$$Q_L = \dot{m} \text{ x } \Delta\omega \text{ x } h \quad (9)$$

$$Q_L = \rho \text{ x } \dot{V} \text{ x } \Delta\omega \text{ x } h \quad (10)$$

Where
$\Delta\omega = \omega_{\text{mixed air}} - \omega_{\text{supply air}}$
$\dot{V}$ = Volumetric air flow rate, m3/s
ρ = the density of air at temperature T, kg/m3
h = latent heat of evaporation in kJ per kg moisture

Table 6 Hourly (9:00AM- 4:00PM) Energy Consumption

CONTROL METHOD	ON/OFF			PID		
	23°C(kWh)	**24°C(kwh)**	**25°C(kWh)**	**23°C(kWh)**	**24°C(kWh)**	**25°C(kWh)**
	18/04/2021	**20/10/2019**	**29/03/2021**	**26/12/2021**	**2/1/2022**	**16/1/2022**
9:00 - 10:00	17.7	18.5	17.8	11.9	10.5	11.0
10:00 - 11:00	18.7	17.9	17.7	11.1	10.4	9.5
11:00 - 12:00	17.5	15.1	17.9	11.8	9.7	10.0
12:00 - 1:00	19.5	19.1	16.8	11.4	10.1	8.7
1:00 - 2:00	17.5	15.4	17.5	11.7	9.81	7.5
2:00 - 3:00	18.6	16.4	12.6	11.4	10.3	9.9
3:00 - 4:00	16.8	13.3	12.5	11.0	9.67	11.0
AVERAGE ENERGY	**18.0**	**16.5**	**16.1**	**11.5**	**10.1**	**9.7**
	19/04/2021	**21/10/2019**	**30/03/2021**	**27/12/2021**	**3/1/2022**	**17/1/2022**
9:00 - 10:00	15.9	16.7	17.3	12.7	10.9	11.0
10:00 - 11:00	16.4	17.2	17.9	11.3	10.0	10.0
11:00 - 12:00	17.6	17.5	17.5	11.6	11.6	9.7
12:00 - 1:00	18.0	15.4	17.8	11.7	9.96	11.0
1:00 - 2:00	18.1	18.4	12.2	11.0	9.0	8.9
2:00 - 3:00	18.1	14.8	10.1	11.1	9.97	7.9
3:00 - 4:00	18.0	14.6	17.7	11.2	8.84	8.5
AVERAGE ENERGY	**17.5**	**16.4**	**15.8**	**11.5**	**10.1**	**9.6**
	20/04/2021	**22/10/2019**	**31/03/2021**	**28/12/2021**	**4/1/2022**	**19/1/2022**
9:00 - 10:00	19.5	16.5	15.9	12.5	10.5	11.0
10:00 - 11:00	15.3	17.2	15.9	11.3	9.02	11.0
11:00 - 12:00	17.3	17.4	15.6	9.54	9.98	10
12:00 - 1:00	17.7	14.6	18.0	9.75	10.7	8.1
1:00 - 2:00	19.2	15.6	15.1	10.9	9.21	7.5
2:00 - 3:00	18.1	15.8	15.1	12.1	10.7	8.5
3:00 - 4:00	18.1	16.7	15	12.3	10.0	10.0
AVERAGE ENERGY	**17.9**	**16.3**	**15.8**	**11.2**	**10.0**	**9.4**
	21/04/2021	**23/10/2019**	**1/4/2021**	**29/12/2021**	**5/1/2022**	**20/1/2022**
9:00 - 10:00	18.0	19.0	15.1	11.9	8.94	9.6
10:00 - 11:00	17.2	16.7	15.1	11.3	9.51	9.4
11:00 - 12:00	17.4	15.6	15.4	12.5	9.84	9.3
12:00 - 1:00	16.6	14.4	17.7	10.4	10.5	9.5
1:00 - 2:00	17.9	16.4	16.1	10.5	8.5	10.0
2:00 - 3:00	17.7	17.2	16.1	11.6	10.6	9.5
3:00 - 4:00	17.7	17.3	16.3	11.9	10.6	8.2
AVERAGE ENERGY	**17.5**	**16.7**	**15.9**	**11.4**	**9.8**	**9.4**
	22/04/2021	**24/10/2019**	**4/4/2021**	**30/12/2021**	**6/1/2022**	**23/1/2022**
9:00 - 10:00	16.6	17.1	14.6	11.9	10.1	9.0
10:00 - 11:00	17.1	16.8	15.1	11.3	10.4	9.5
11:00 - 12:00	17.3	15.1	16.3	10.6	10.4	8.8
12:00 - 1:00	17.2	18.3	15.2	10.7	10.6	8.7
1:00 - 2:00	19	17.3	16.3	10.8	10.8	9.5
2:00 - 3:00	17.7	16.3	17.1	11.1	10.8	9.3
3:00 - 4:00	18.1	15.1	16.9	12.0	10.9	11.0
AVERAGE ENERGY	**17.6**	**16.6**	**15.9**	**11.2**	**10.5**	**9.4**

Table 7 Average Daily Coefficient of Performance

CONTROL METHOD	ON/OFF			PID		
	23°C	24°C	25°C	23°C	24°C	25°C
	18/04/2021	**20/10/2019**	**29/03/2021**	**26/12/2021**	**2/1/2022**	**16/1/2022**
9:00 - 10:00	2.3	2.4	2.9	4.3	4.5	5.4
10:00 - 11:00	2.6	2.5	3.2	4.1	4.5	4.1
11:00 - 12:00	2.7	2.7	3.2	4.3	4.7	4.7
12:00 - 1:00	2.6	2.7	3.3	4.1	4.6	5.2
1:00 - 2:00	2.6	2.8	3.0	4.0	4.4	5.1
2:00 - 3:00	2.5	3.0	2.8	4.0	4.3	4.2
3:00 - 4:00	2.3	3.0	3.2	4.1	4.5	4.8
AVERAGE COP	**2.5**	**2.7**	**3.1**	**4.1**	**4.5**	**4.8**
	19/04/2021	**21/10/2019**	**30/03/2021**	**27/12/2021**	**3/1/2022**	**17/1/2022**
9:00 - 10:00	2.5	2.5	3.1	4.2	3.9	4.5
10:00 - 11:00	3.0	3.0	3.6	4.1	4.3	4.7
11:00 - 12:00	2.3	2.9	3.3	4.0	3.7	4.2
12:00 - 1:00	2.9	2.7	3.3	4.3	4.4	4.6
1:00 - 2:00	2.4	3.2	2.3	4.3	4.7	4.9
2:00 - 3:00	2.3	2.4	2.8	4.3	4.4	5.7
3:00 - 4:00	2.9	2.8	3.3	4.2	4.8	6.1
AVERAGE COP	**2.6**	**2.8**	**3.1**	**4.2**	**4.3**	**5.0**
	20/04/2021	**22/10/2019**	**31/03/2021**	**28/12/2021**	**4/1/2022**	**19/1/2022**
9:00 - 10:00	2.7	2.5	3.3	4.2	4.2	4.9
10:00 - 11:00	2.6	2.4	3.1	4.1	4.9	4.9
11:00 - 12:00	2.3	2.3	3.1	4.0	4.4	4.2
12:00 - 1:00	2.7	2.9	3.4	4.4	4.2	4.3
1:00 - 2:00	2.3	2.7	3.4	4.1	4.7	4.9
2:00 - 3:00	2.6	3.3	3.2	4.2	5.0	5.1
3:00 - 4:00	2.6	2.6	3.3	4.2	4.4	4.9
AVERAGE COP	**2.5**	**2.7**	**3.2**	**4.2**	**4.5**	**4.7**
	21/04/2021	**23/10/2019**	**1/4/2021**	**29/12/2021**	**5/1/2022**	**20/1/2022**
9:00 - 10:00	2.5	2.8	3.2	4.3	4.1	4.5
10:00 - 11:00	2.7	3.0	3.3	4.2	4.7	4.4
11:00 - 12:00	2.6	3.2	2.8	3.4	4.6	5.2
12:00 - 1:00	2.8	3.3	3.5	4.1	4.4	4.3
1:00 - 2:00	2.6	2.9	3.7	4.0	4.2	4.8
2:00 - 3:00	2.6	2.6	3.4	4.0	4.3	4.3
3:00 - 4:00	2.6	2.9	2.9	4.1	4.4	4.3
AVERAGE COP	**2.6**	**3.0**	**3.3**	**4.0**	**4.4**	**4.6**
	22/04/2021	**24/10/2019**	**4/4/2021**	**30/12/2021**	**6/1/2022**	**23/1/2022**
9:00 - 10:00	2.2	2.8	3.2	4.2	4.5	5.2
10:00 - 11:00	2.2	2.4	3.7	4.1	4.4	4.7
11:00 - 12:00	3.2	2.7	3.3	4.0	4.4	4.2
12:00 - 1:00	3.1	2.7	3.5	4.4	4.3	4.3
1:00 - 2:00	2.7	2.7	3.4	4.3	5.1	5.2
2:00 - 3:00	2.1	3.1	3.1	4.1	4.3	5.6
3:00 - 4:00	2.3	3.4	2.9	4.2	4.3	4.3
AVERAGE COP	**2.5**	**2.8**	**3.3**	**4.2**	**4.5**	**4.8**

Figure 17 and 18 shows the graphical representations of the average coefficient of performance at all the setpoints of 23°C, 24°C, 25°C. it can be observed from the tables above and figure 17 and 18 that the COP has the best improvement with the implementation of the PID.

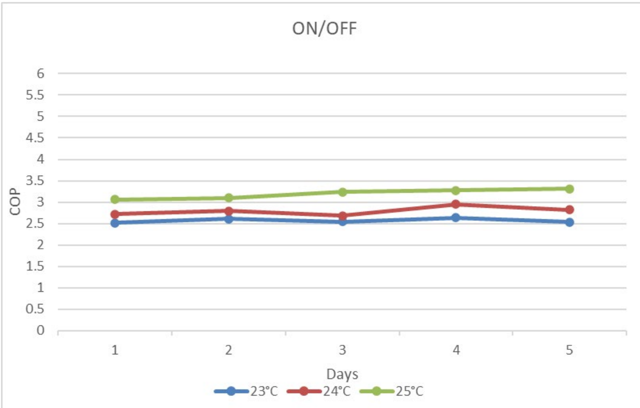

Figure 17 Effect of setpoint on COP using ON/OFF control

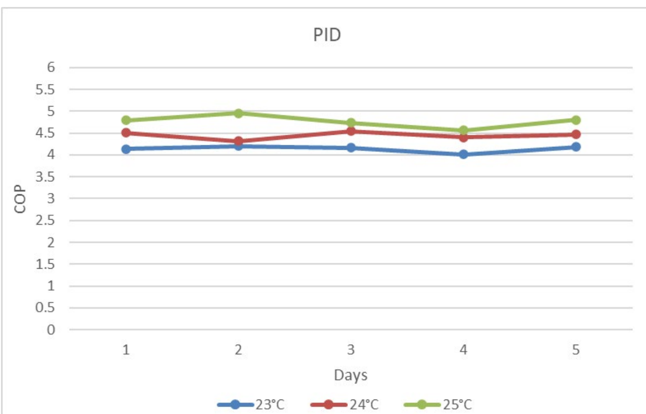

Figure 18 Effect of setpoint on COP using PID control

C. Temperature Setpoint Tracking

In temperature control applications a setpoint is the target value at which a controller attempts to maintain the process variable [20]. This can be achieved by adjusting its control output power. The ability of the controller to maintain the setpoint means good management of energy consumption and thermal comfort for indoor inhabitant. It can be observed from figure 19 that the On/Off controller could not maintain the indoor temperature setpoint of 23°C at the desired level. The setpoint was fluctuating at different points between 20°C to 24°C, most time reducing to 20°C. This happens because of the inefficient strategy of the On/Off thermostat control. This inefficiency arises as a result of the fact that the On/Off thermostat control uses return air as the control feedback. But the return air does not accurately represent the current temperature setting of the indoor, thus the controller assumes a higher indoor air temperature and this makes the two-compressor run almost all the time resulting in overcooling and excessive energy consumption.

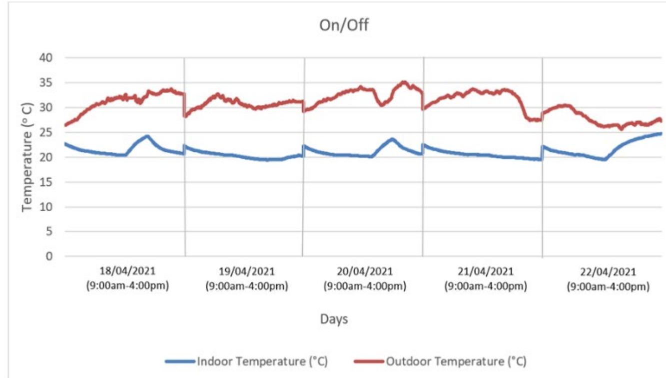

Figure 19 Effect of On/Off Control On Setpoint Tracking

Figure 20 shows the effect the PID has on maintaining the indoor temperature setpoint, it shows that the indoor temperature was maintained at the required setpoint.

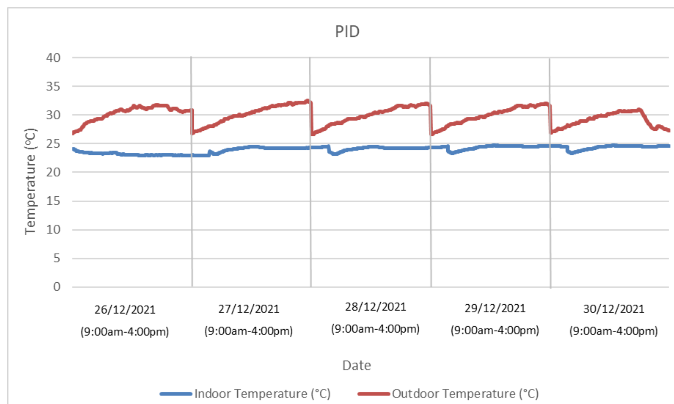

Figure 20 Effect of PID on setpoint tracking

This study has shown that the PID strategy is effective in maintaining the setpoint of the multi-circuit centralized air conditioning systems due to its ability to provide precise, stable, and adaptive control. By addressing current, and past errors, it ensures the temperature remains consistent with the setpoint, enhancing comfort and energy efficiency. The PID controller minimizes oscillations around the setpoint and provides rapid correction of variations in temperature due to its potential combination of proportional, integral, and derivative actions. The outdoor air temperature affects the heat transfer through external walls and roofs as well as the heat transfer by ventilation. Outdoor air temperature is a driving force for natural ventilation and studies have indicated that building energy consumption is intimately tied to changes in outdoor temperature, and such relationships between the two is very significant. The graphs shown in Figures 19 and 20 above indicates that the outdoor conditions for both control method are similar and as such the basis for comparison of energy consumption between the controllers is justified. Setting and maintaining the indoor temperature at 23°C effectively satisfies thermal comfort for most individuals by adhering to international comfort standards, aligning with human thermal neutrality, and supporting both personal well-being and building energy performance [21].

4.0 CONCLUSION

The main focus of this study is on energy reduction in a multi-circuit centralized air-cooled air conditioning system. The impact of PID and the variable frequency drive on the performance of the system has been demonstrated. It has significantly impacted on energy consumption, coefficient performance, and setpoint tracking. The performance of the controller was put to test on the multi-circuit centralized air conditioning system. For the purpose of comparison, the energy savings was calculated before and after the implementation of PID at three different setpoints. It was observed that at all temperature setpoints, the PID performed better than On/Off. The Coefficient of Performance (COP) of the air conditioning system also improved significantly after the controller's installation compared to the On/Off thermostat control operation. By operating within close range temperature bands as indicated in the PID algorithm thus avoiding unnecessary cooling, the setpoint was also well tracked. Therefore, it has been demonstrated that the combination of PID and variable frequency drive ensures that the system operates more efficiently, thus reducing energy consumption contributing to improved COP and effective indoor temperature setpoint tracking. This study has contributed towards the knowledge of strategies for the reduction in energy consumption and improvement in the COP of an operational multi-circuit centralized air-cooled air conditioning system. This research study has developed an energy saving strategy for an operational multi-circuit centralized air-cooled air conditioning system. It has also led to opportunities for future improvements. Future works may consider the recommendations below:

(a) Considering the effect of variable frequency drive on indoor room air temperature and energy consumption which has been established in this study, there is a need for further research in monitoring and controlling the air quality index such as the indoor CO2 level. Therefore, further research can determine the impact of the energy saving strategy on the indoor air quality.

(b) Another major parameter that affects indoor thermal comfort is humidity. In further studies on operational multi-circuit air conditioning system, both temperature and humidity control could be considered.

Acknowledgement

This work was supported by the Ministry of Higher Education Malaysia and Universiti Teknologi Malaysia through the Translational Research Grant (UTM-TRG) Vot 4J337.

Conflicts of Interest

The authors declare that there is no conflict of interest regarding the publication of this paper.

References

[1] Özahi, E., A. Abuşoğlu, A. İ. Kutlar, and O. Dağcı. 2017. A Comparative Thermodynamic and Economic Analysis and Assessment of a Conventional HVAC and a VRF System in a Social and Cultural Center Building. *Energy and Buildings.* 140: 196–209. https://doi.org/10.1016/j.enbuild.2017.02.008.

[2] Abdullah, H., O. Ibrahim, M. N. M. Jaafar, M. Maziah, and S. Sulaiman. 2020. Energy Savings in a Multi-Circuit Water-Cooled Packaged Unit Air-Conditioning System. 76(1).

[3] Abu Bakar, N. N., *et al.* 2015. Energy Efficiency Index as an Indicator for Measuring Building Energy Performance: A Review. *Renewable and Sustainable Energy Reviews.* 44: 1–11. https://doi.org/10.1016/j.rser.2014.12.018.

[4] Mohammed, A., A. Mustapha, and N. Mu'azu. 2011. Energy Efficient Buildings as a Tool for Ensuring Sustainability in the Building Industry. In *2011 International Conference on Multimedia Technology*. 4402–4405. https://doi.org/10.1109/ICMT.2011.6003238.

[5] Oleolo, I., H. Abdullah, M. Mohamad, and M. N. M. Jaafar. 2020. Model Selection for the Control of Temperature in a Centralized Air Conditioning System. *Journal of Advanced Research in Applied Mechanics.* 74(1): 10–20. https://doi.org/10.37934/aram.74.1.10207.

[6] Yang, Z., A. Ghahramani, and B. Becerik-Gerber. 2016. Building Occupancy Diversity and HVAC (Heating, Ventilation, and Air Conditioning) System Energy Efficiency. *Energy.* 109: 641–649. https://doi.org/10.1016/j.energy.2016.04.099.

[7] Afram, A., and F. Janabi-Sharifi. 2014. Review of Modeling Methods for HVAC Systems. *Applied Thermal Engineering.* 67(1): 507–519. https://doi.org/10.1016/j.applthermaleng.2014.03.055.

[8] Jouhara, H., and J. Yang. 2018. Energy Efficient HVAC Systems. *Energy and Buildings.* 179: 83–85. https://doi.org/10.1016/j.enbuild.2018.09.001.

[9] Farinaz, B., R. R. Abdul, S. Khairulmizam, and E. Hossein. 2017. Energy Saving by Applying the Fuzzy Cognitive Map Control in Controlling the Temperature and Humidity of Room. *International Journal of Physical Sciences.* 12(1): 13–23. https://doi.org/10.5897/IJPS11.822.

[10] Oleolo, I., H. Abdullah, M. Mohamad, M. N. M. Jaafar, A. Baharain, and S. Sulaiman. 2021. Model Analysis for the Control of Humidity in a Water-Cooled Centralized Air Conditioning System. *Journal of Advanced Research in Fluid Mechanics and Thermal Sciences.* 80(2): 1–12.

[11] Jönsson, I. Synnøve. 2015. System Identification for Control of Temperature and Humidity in Buildings. Accessed March 13, 2025. https://lup.lub.lu.se/student-papers/search/publication/7440340.

[12] Zimmermann, M., H.-J. Althaus, and A. Haas. 2005. Benchmarks for Sustainable Construction: A Contribution to Develop a Standard. *Energy and Buildings.* 37(11): 1147–1157.

[13] Oleolo, I., *et al*. n.d. Long Short-Term Memory Neural Network Model for the Control of Temperature in a Multi-

Circuit Air Conditioning System. Accessed March 15, 2025. https://www.researchgate.net/profile/Balogun-Adebayo/publication/372287900.

[14] Zhong, Z., X. Xu, X. Zhang, and Z. Huang. 2017. Simulation Based Control Performance Evaluation of a Novel Fuzzy Logic Control Algorithm for Simultaneously Controlling Indoor Air Temperature and Humidity Using a Direct Expansion (DX) Air-Conditioning (A/C) System. *Procedia Engineering*. 205: 1792–1799.

[15] Lam, J. C., C. L. Tsang, and L. Yang. 2006. Impacts of Lighting Density on Heating and Cooling Loads in Different Climates in China. *Energy Conversion and Management*. 47(13–14): 1942–1953.

[16] Vakiloroaya, V., B. Samali, A. Fakhar, and K. Pishghadam. 2014. A Review of Different Strategies for HVAC Energy Saving. *Energy Conversion and Management*. 77: 738–754. https://doi.org/10.1016/j.enconman.2013.10.023.

[17] Samuel, M., M. Mohamad, M. Hussein, and S. M. Saad. 2021. Lane Keeping Maneuvers Using Proportional Integral Derivative (PID) and Model Predictive Control (MPC). *Journal of Robotics and Control (JRC)*. 2(2): 78–82.

[18] Abioye, A. E., *et al.* 2023. Model Based Predictive Control Strategy for Water Saving Drip Irrigation. *Smart Agricultural Technology*. 4: 100179.

[19] ASHRAE. 2005. *ASHRAE Handbook—Fundamentals (SI Edition)*. Atlanta, GA: American Society of Heating, Refrigerating and Air-Conditioning Engineers.

[20] Samuel, M., M. Maziah, M. Hussien, and N. Y. Godi. 2018. Control of Autonomous Vehicle Using Path Tracking: A Review. *Advanced Science Letters.* 24(6): 3877–3879.

[21] de Dear, R. J., and G. S. Brager. 2002. Thermal Comfort in Naturally Ventilated Buildings: Revisions to ASHRAE Standard 55. *Energy and Buildings.* 34(6): 549–561.